agriculture

MDPI

Article

Sensitivity Analysis of N_2O and CH_4 Emissions in a Winter Wheat–Rice Double Cropping System

Chuang Liu [1,2,*,†], Jiabao Wang [1,†], Zhili Sun [1], Yixiang Sun [1,*], Yi Liu [2] and Lianhai Wu [3,4]

[1] Key Laboratory of Nutrient Cycling Resources and Environment of Anhui, Institute of Soil and Fertilizer, Anhui Academy of Agricultural Sciences, Hefei 230001, China; wangjiabao@aaas.org.cn (J.W.); zhilisun@ahstu.edu.cn (Z.S.)
[2] Key Laboratory of Aquatic Botany and Watershed Ecology, Wuhan Botanical Garden, Chinese Academy of Sciences, Wuhan 430074, China; liuyi@wbgcas.cn
[3] Rothamsted Research, North Wyke, Okehampton, Devon EX20 2SB, UK; lianhai.wu@rau.ac.uk
[4] School of Agriculture, Food and the Environment, Royal Agricultural University, Gloucestershire GL7 6JS, UK
* Correspondence: liuchuang@wbgcas.cn (C.L.); sunyixiang@aaas.org.cn (Y.S.)
† These authors contributed equally to this work.

Abstract

The sensitivity of model outputs to parameter variations is crucial for effective model calibration and application. This study assessed the sensitivity of N_2O and CH_4 emissions to varying weather conditions and fertilization practices in a winter wheat–rice cropping system. Using the Sobol first-order sensitivity index within the SPACSYS model, key parameters and input variables influencing gas emissions were identified. The results showed that the index effectively detected highly sensitive parameters, particularly those related to soil water content, oxygen dynamics and microbial processes. Both N_2O and CH_4 emissions were sensitive to carbon availability and soil oxygen levels. For N_2O emissions, microbial process parameters and soil water content had substantial impacts, whereas CH_4 emissions were more responsive to methane consumption, oxygen levels, and carbon substrates. Fertilization, rainfall and temperature showed high sensitivity for N_2O emissions, while temperature emerged as the dominant factor controlling CH_4 emissions. The identified parameters offer valuable insights for improving model performance and informing strategies to mitigate greenhouse gas emissions.

Keywords: SPACSYS; double cropping system; Sobol sensitivity analysis; gas emissions

1. Introduction

Nitrous oxide (N_2O) and methane (CH_4) emissions from agricultural fields are major components of the greenhouse gases (GHGs) responsible for global environmental problem [1,2]. Although the winter wheat–rice double-cropping system maximizes land use efficiency by producing two crops annually and supports food security and economic returns [3], it is also identified as a substantial source of N_2O and CH_4 emissions in China [4]. Thus, understanding and mitigating these emissions is essential for promoting sustainable agricultural development.

Considerable amounts of N_2O and CH_4 are produced in this system due to alternating aerobic and anaerobic soil conditions [5,6]. N_2O emissions originate primarily from two soil microbial processes, nitrification and denitrification, both of which are influenced by soil water content (SWC), temperature, organic matter (OM) content, and agronomic practices [7–9]. Excessive nitrogen (N) fertilization can increase the availability of substrates

Received: 9 October 2025
Revised: 11 December 2025
Accepted: 17 December 2025
Published: 19 December 2025

for these microbial processes, thereby enhancing N_2O emissions [10]. Under anaerobic paddy conditions, CH_4 is generated by methanogenic archaea that consume acetate or CO_2 as substrates, facilitated by the enzyme methyl-coenzyme M reductase [11,12]. However, accurately measuring in situ N_2O and CH_4 emissions across spatial and temporal scales remains challenging [13]. Rapid fluctuations in SWC, temperature, and OM content can cause substantial changes in gas production [14]. Traditional measurement techniques often lack the temporal and spatial resolution needed to capture these variations, resulting in knowledge gaps concerning GHG spatiotemporal variability [15,16]. These limitations underscore the necessity of advanced modelling approaches that can simulate gas fluxes under diverse environmental and management conditions.

Mathematical models are widely used to explore the impacts of environmental conditions and management practices (e.g., water and fertiliser management, tillage) on N_2O and CH_4 production and dissipation, as well as the interactions between crop, soil and environment [17]. The SPACSYS model is one such sophisticated tool designed to simulate soil–plant–atmosphere interactions; it can reliably predict crop growth, soil hydrology, nutrient cycling, and GHG emissions in complex agroecosystems [18,19]. Briefly, SPACSYS integrates microbial and chemical processes associated with nitrification and denitrification processes for N_2O production and the entire methanogenesis pathway, including CH_4 oxidation by methanotrophs, diffusion, plant mediated transport, and ebullition [19]. Previous studies have applied SPACSYS to assess crop production and GHG emissions to agronomic management and climate change in both arable and grassland ecosystems across diverse soil types and climatic regions [20–22].

Process-based models often incorporate numerous parameters associated with considerable uncertainties, leading to variability in model predictions [23]. Understanding the sensitivity of model outputs to parameters variations is therefore essential for effective model calibration, as it helps identify and prioritise the most influential parameters [24]. Sensitivity analysis (SA) serves as a vital tool for this purpose, allowing both qualitative and quantitative assessments of how input variables and parameters affect model outputs [25]. By focusing on these parameters identified as most sensitive, users can streamline the calibration process and improve overall model performance and reliability [24].

Sensitivity analysis techniques can generally be categorized as local and global. Global SA quantifies how output uncertainty can be apportioned to multiple sources of input uncertainty [26], whereas local SA, typically a one-at-a-time (OAT) technique, focuses on the primary (first-order) effects of individual input variables on model outputs while holding all others constant [27]. Local SA is particularly effective for linear or near-linear systems, as it isolates individual parameter effects.

A previous sensitivity analysis of SPACSYS based on data from a winter wheat field experiment examined 61 parameters across 27 output variables [28]. That study identified the maximum autotrophic nitrification rate, the fraction of NO produced during nitrification, and the Q10 temperature coefficient for denitrification as the most sensitive parameters affecting the N_2O emission rate in upland soil. Since the CH_4 dynamics module was incorporated into SPACSYS after that study, no SA has yet been performed for CH_4 emissions. Consequently, a comprehensive SA of both N_2O and CH_4 emissions in paddy–upland cropping systems remains lacking. Compared with earlier modelling efforts, SPACSYS's integrated structure, which simulates soil–plant–atmosphere interactions and coupled carbon (C)–N cycling, enables the model to capture feedbacks among soil physicochemical conditions, crop growth, and N transformations, providing a robust framework for identifying key parameters driving GHG emissions.

The SPACSYS model has been calibrated and validated with the dataset from the experiment that underpins this study [29]. Here, we conducted a comprehensive SA involv-

ing that included 65 parameters related to soil C and N cycling and water movement, 21 soil properties, and two representative weather scenarios (each including five levels of rainfall and temperature). We employed the classic Sobol first-order sensitivity index (SFI) within a local SA framework to quantify the sensitivity of key parameters in SPACSYS model. The primary objective of this study was to identify the parameters that govern variability in N_2O and CH_4 emissions in the winter wheat–rice cropping system, thereby improving the robustness of SPACSYS through targeted SA. Specifically, we aimed to (1) assess how variations in weather conditions and fertilization practices influence N_2O and CH_4 emissions; (2) to identify the most influential parameters affecting N_2O and CH_4 emissions; and (3) to refine model calibration by prioritizing these critical parameters.

2. Materials and Methods

2.1. Study Site

The experimental dataset from a winter wheat–rice cropping system was used for this study. The field experiment was conducted between 2020 and 2023 in a subtropical humid monsoon climate zone in He County, located in the lower Yangtze River Basin in China (31°46′ N, 118°12′ E, 18 m a.s.l.). The average annual temperature and rainfall in the region are 15.8 °C and 1067 mm, respectively. The soil at the experiment site was classified as *Hydragric Anthrosols* based on the World Reference Base for Soil Resources (WRB) system [30], corresponding broadly to *Anthraquolls* or *Aquepts* in the USDA Soil Taxonomy. At the beginning of the experiment, initial soil physical and chemical properties were measured for the 0–60 cm soil layer (Table 1).

Table 1. Initial soil physical and chemical properties at different soil depths at the experimental site in October 2020.

Depth	Clay	Silt	Sand	BD	pH	SOM	TN
(cm)	(%)	(%)	(%)	(g cm^{-3})		(g kg^{-1})	(g kg^{-1})
0–20	20.8	63.4	15.8	1.19	6.0	14.8	1.07
20–40	18.1	63.5	18.4	1.53	6.4	10.6	–
40–60	17.9	54.6	27.5	1.53	6.4	6.2	–

Note: BD, bulk density; SOM, soil organic matter; TN, soil total N.

Winter wheat and rice rotation is a typical cropping system in this region, with winter wheat grown under rainfed conditions and rice grown under irrigation, receiving approximately 500 mm over the whole growing season. Local cultivars of wheat (‘*Zhenmai 12*’) and rice (‘*Fuxiangzhan*’) were used, along with standard field management practices including tillage, weed and pest control. Before sowing or transplanting, each plot was tilled to a depth of 20 cm using a field cultivator to prepare the seedbed. Winter wheat was sown in early November and harvested in late May, followed by transplanting in mid-June and harvesting in late September. The plot size for both crops was 40 m × 40 m.

2.2. The SPACSYS Model

The overall structure of SPACSYS includes the coupling of soil C–N cycling, plant growth, and water–heat transfer modules, following the standard framework described in the SPACSYS manual [18–20,31]. Here, we briefly summarise the processes related to GHG emissions. The nitrification process considers the autotrophic pathway involving a series of microbial evolution and response functions governed by substrate availability and soil environmental conditions. Denitrification is modelled as a sequential reduction of nitrate to gaseous N compounds under anaerobic conditions. For CH_4 dynamics, the model integrates major processes, including methane production, oxidation, diffusion,

plant-mediated uptake and transport, and ebullition. Methane oxidation is calculated as a function of soil temperature, moisture, gas diffusivity, substrate concentration, and methanotrophic inhibition [32]. Methane production is estimated based on the sensitivity of methanogenesis to O_2 inhibition [33], while plant-mediated CH_4 transport and ebullition are modelled based on gas diffusion driven by partial pressure gradients [34].

2.3. Sensitivity Analysis Design

To evaluate the sensitivity of N_2O and CH_4 emissions simulated by SPACSYS, we examined how variations in weather conditions, soil properties, fertilization practices, and key model parameters governing soil C–N cycling and water movement influence model outputs.

2.3.1. Weather Conditions

Historical daily weather data were served as the baseline for simulations. To analyse the impacts of changing weather conditions on model outputs, we conducted simulations in which the average temperature and rainfall were increased or decreased by 10%, 20% and 30% relative the historical values.

2.3.2. Soil Property Settings

Ten soil physical variables plus pH were adjusted by ±50% from their default values (Table 2). Each variable was sampled 100 times, resulting in a total of 1100 simulations to evaluate the influence of soil property variations on model outputs [28].

Table 2. Soil physical and chemical variables, their abbreviation and default values at the depths of 0–10 cm and 10–20 cm during the sensitivity simulation period.

Description	0–10 cm		10–20 cm	
	Abbreviation	**Value**	**Abbreviation**	**Value**
pH value (-)	PHL1	6.36	PHL2	6.4
Air entry pressure (cm water)	AEPL1	46.8	AEPL2	46.2
Pore size distribution index (-)	PSDIL1	0.31	PSDIL2	0.35
Macro pore volume (vol%)	MPVL1	4	MPVL2	6.3
Saturated total conductivity (mm day^{-1})	TKSL1	743	TKSL2	1060
Saturated matrix conductivity (mm day^{-1})	SMCL1	22.4	SMCL2	22.4
Water content at wilting point (vol%)	WPL1	13.3	WPL2	7.9
Field capacity (vol%)	FCL1	27.2	FCL2	22.5
Saturated water content (vol%)	SSCL1	45.4	SSCL2	39.5
Residue water content (vol%)	RSWCL1	6.8	RSWCL2	4.1
Dry soil bulk density (g cm^{-3})	DSBDL1	1.19	DSBDL2	1.19

2.3.3. Fertilization Practices

Fertilization practices involved applying urea (46% N) at rates of 150 and 180 kg N ha^{-1} for wheat and rice, respectively, following standard local management practices. To quantify the sensitivity of model outputs to fertilization practices and their impact on GHG emissions, we evaluated several fertiliser application strategies, while keeping total N rates consistent with the same as the field experiment. These included basal application plus topdressing at tillering with ratios of 70:30 (R7:3), 60:40 (R6:4) and 50:50 (R5:5), as well as basal application combined with topdressings at tillering and heading with ratios of 40:30:30 (R4:3:3) and 50:30:20 (R5:3:2).

2.3.4. Model Required Parameters on Water, C and N Processes

Sixty-five parameters related to water distribution, nitrification and denitrification, methane dynamics were considered (Table S1). Each parameter range was set to ±50% of its default value. To ensure uniform coverage across the entire probability distribution, each parameter was sampled 100 times, resulting in a total of 6500 simulations.

2.4. The Sobol's First-Order Method for Sensitivity Diagnostics

The Sobol's first-order index provides a non-parametric measure of the individual contributions of input variables to the variance of model outputs, enabling a comprehensive assessment of their relative importance. In this study, we leverage SFI to unravel the intricate relationships between parameters or input variables and their influence on simulation output variables. This approach provides valuable insights into the key factors driving the behaviour of simulation output variables. SFI is defined as [35]:

$$SFI = (V[E(Y \mid X_i)])/(V(Y))$$

where V is the partial variance associated with the main effect of input variable X_i(I = 1, 2, . . . , 100); $V(Y)$ is the total unconditional variance of the output Y; and $E(Y \mid X_i)$ represents the expected value of Y conditional on a fixed value of X_i. A higher SFI indicates that variation in a factor has a greater impact on output variance. Generally, a model output is considered sensitive to a parameter if its corresponding SFI > 0.1 [35]. In this study, we employed SFI to unravel the relationships between parameters or input variables and their influence on simulation outputs, providing insights into the key factors driving model behaviour.

SFI was calculated using the variance estimators implemented in the 'sensitivity' package in R software (ver. 4.2). The '*sobol()*' function, combined with the *Saltelli* sampling scheme, was used to generate input matrices, and the '*tell()*' function was applied to incorporate model outputs and derive the first-order indices.

3. Results

N_2O and CH_4 emissions from the cropping system were significantly influenced by the selected parameters and input variables, with SFI values > 0.1, as shown in Figure 1. Emissions were insensitive to 39 and 41 of the 65 parameters for N_2O and CH_4, respectively, as their SFI values were below 0.1. These emissions were particularly insensitive to parameters primarily related to soil properties. Reducing the transformation of fresh litter or OM to dissolved C could decrease both N_2O and CH_4 emissions.

3.1. Fertilisation and Weather Impacts on N_2O and CH_4 Emissions

Cumulative N_2O and CH_4 emissions under different levels of basal/topdressing, rainfall and temperature during the growing season of the crops varied (Figure 2). A higher proportion of topdressing (i.e., R4:3:3 and R6:2:2) increased accumulated N_2O emissions by ca. 53%, while CH_4 emissions under different basal/topdressing ratios showed only slight fluctuations (<5%, Figure 2a). Among the climatic variables, the simulated emission patterns of annual N_2O and CH_4 emissions varied under different rainfall and temperature conditions. N_2O emissions showed a biphasic response to increased rainfall, initially rising by 0.24 g N m^{-2} day^{-1} before declining as rainfall continued (Figure 2b). In contrast, CH_4 emissions displayed a slight initial reduction, followed by an increase with changing rainfall, likely due to the automatic irrigation practice during the rice growing period. The effect of warmer temperature on N_2O exhibited a pattern where emissions decreased by ca. 30% initially, then increased by 0.22 g N m^{-2} day^{-1}. This response can be attributed to the complex interactions between temperature and soil processes, where lower temperatures initially reduce microbial activity and nitrification rates, leading to lower N_2O emissions.

However, as temperatures rise, enhanced soil microbial activity and accelerated N mineralization, likely contribute to increased N_2O emissions. In contrast, the effect of warmer temperatures on CH_4 emissions was generally positive (*ca*. 239%, Figure 2c), largely due to increased availability of soil C pools resulting from enhanced soil mineralization.

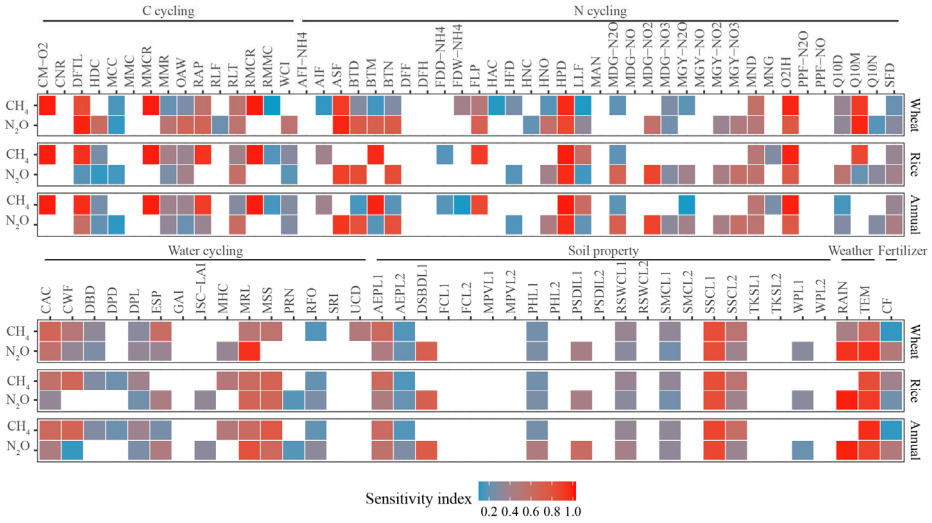

Figure 1. Heatmap of SFI for input variables and parameters influencing simulated N_2O and CH_4 emissions during the wheat and rice growing periods, as well as over the entire year. White pixels indicate no significant interaction (SFI < 0.1).

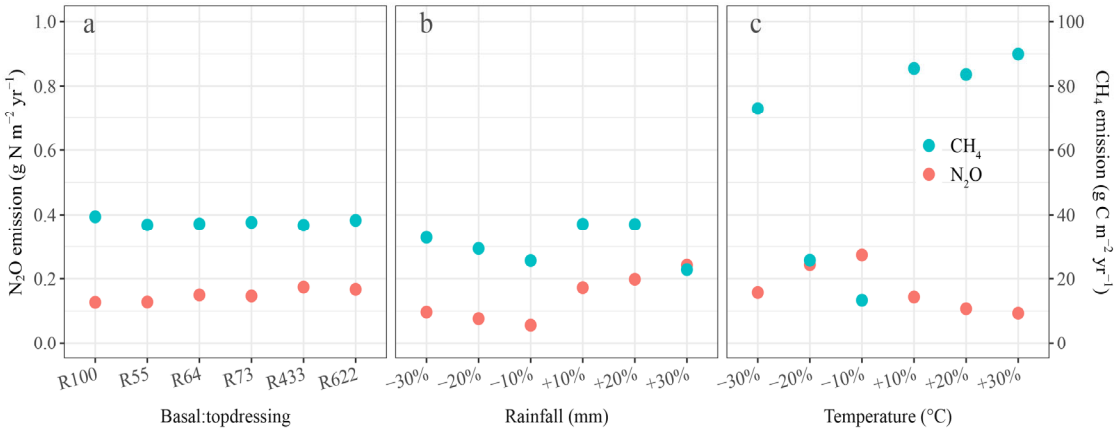

Figure 2. Changes in annual N_2O and CH_4 emissions under different levels of basal/topdressing ratios (**a**), rainfall (**b**) and temperature (**c**) in a winter wheat–rice cropping system over the simulation period.

3.2. Relationships Between Simulated N_2O and CH_4 Emissions and Model Processes Parameters

3.2.1. Parameters in Soil Nitrogen Cycling

The changes in N_2O and CH_4 emissions with significant sensitivity parameters related to soil nutrient and microorganisms are shown in Figure 3. N_2O emissions were highly sensitive to the assimilation factor (ASF) and humus potential decomposition rate (HPD) and (Figure 3a,d), while an increase in the base temperature at which the temperature function is in unity for denitrification and nitrification (BTD and BTN), and half NO_x concentration (HNO) notably reduced emissions (Figure 3b,f). Increases in BTD, BTN and Q10 for denitrification and nitrification (Q10D and Q10N) led to a reduction in emissions (Figure 3b,c), while higher specific fertiliser dissolution rates (SFD) and the base temperature at which the temperature function is in unity for mineralization (BTM) notably promoted emissions

(Figure 3a,b). In contrast, the litter unit loss fraction (LLF) and humus fraction from dissolved OM (HFD) exhibited only moderate impacts on emissions (Figure 3a). Furthermore, we presented detailed results for parameters related to nitrifier and denitrifier dynamics to examine the contribution of microorganisms to N_2O emissions. These parameters include the maximum nitrifier growth rate (MNG), the maximum nitrifier death rate (MND), the maximum growth yield (MGY-N_2O, MGY-NO, MGY-NO_2 and MGY-NO_3), the NO and N_2O production fractions from the nitrification process (PPF-NO and PPF-N_2O) and the maximum $N_2O/NO_2/NO_3$ denitrifier growth rates (MDG-$N_2O/NO_2/NO_3$). The simulated N_2O emission rate was most sensitive to changes in MDG-N_2O (Figure 3b). Increases in MGY-NO_3, MGY-NO_2 and MND resulted in a reduced emissions (Figure 3a,c). In contrary, emissions increased with higher MGY-N_2O, MDG-N_2O and MDG-NO_3 which are related to the yield rate of N_2O and the turnover rate of denitrifiers (Figure 3a,c).

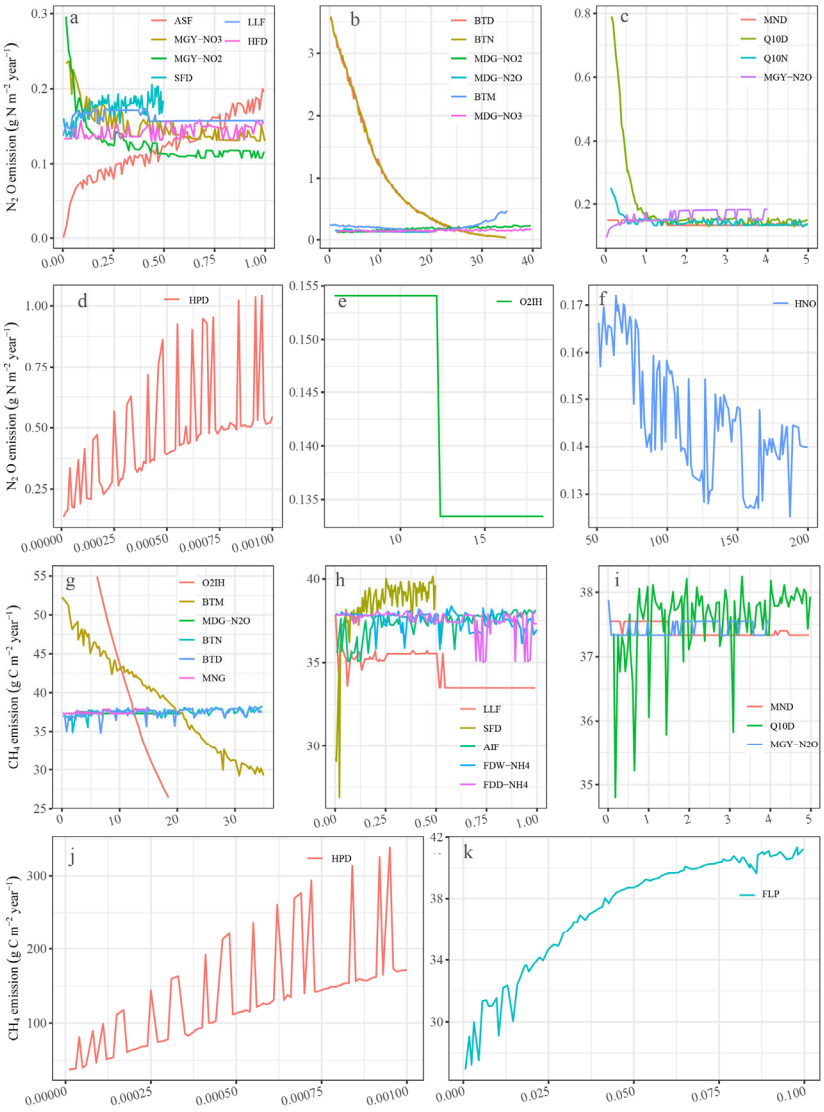

Figure 3. Relationship of N_2O and CH_4 emissions to various parameters: (**a**) OM turnover and denitrifier growth yield related parameters, assimilation factor (ASF), maximum growth yield on NO_3 and NO_2 (MGY-NO_3 and MGY-NO_2), specific fertiliser dissolved rate (SFD), litter loss fraction

(LLF), humus fraction from dissolved OM (HFD); (**b**) temperature-related and denitrifier growth parameters, maximum denitrifier growth rates on NO_2^-, N_2O, and NO_3^- (MDG-NO_2, MDG-N_2O, and MDG-NO_3), base temperature for denitrification and nitrification (BTD and BTN), and base temperature for mineralization (BTM); (**c**) microbial kinetic and temperature sensitivity parameters, maximum nitrifier death rate (MND), maximum denitrifier growth yield on N_2O (MGY-N_2O), and Q10 for nitrification and denitrification (Q10N and Q10D); (**d**) humus potential decomposition rate (HPD); (**e**) oxygen inhibition (O_2IH); (**f**) half-saturation concentration for NOx (HNO); (**g**) temperature- and oxygen-related parameters, BTM, O_2IH, maximum nitrifier growth rate (MNG), MDG-N_2O, and BTN and BTD; (**h**) N and OM input–related parameters, LLF, ammonium immobilized fraction (AIF), SFD and NH_4^+ fraction in wet and dry deposition (FDW-NH_4 and FDD-NH_4); (**i**) microbial kinetic parameters, MND, Q10D, and MGY-N_2O; (**j**,**k**) humus and litter decomposition parameters, HPD and fresh litter potential decomposition rate (FLP).

The humus potential decomposition rate (HPD) and the fresh litter potential decomposition rate (FLP) significantly impacted on CH_4 emissions (Figure 3g,h), with higher BTN, BTD, ammonium immobilized fractions (AIF), SFD and Q10D values resulting in increased emissions (Figure 3g–i). Higher values for oxygen inhibition (O_2IH) and BTM values significantly reduced CH_4 emission (Figure 3g). In contract, MDG-N_2O, MNG, the litter loss fraction (LLF), AIF, NH_4 fractions in wet and dry deposition (FDW-NH_4 and FDD-NH_4), MND and MGY-N_2O had less effect on emissions (Figure 3g,i).

3.2.2. Parameters in Soil Carbon Cycling

We found that eight and eleven of parameters related to soil C processes have significant impacts on annual N_2O and CH_4 emissions (Figure 4). Simulations of N_2O emissions were most sensitive to residue to the residue to litter transfer rate (RLT), where a clear increasing trend in sensitivity was observed (Figure 4a). Higher values for DFTL, MMR, relative activity at porosity (RAP), OAW, HDC and WCI, notably reduced in emissions (Figure 4a,b), while MCC had a lesser impact on emissions (Figure 4c).

Similarly, DFTL, CM-O_2, MMCR and the rhizospheric maximal methane consumption rate (RMCR) significantly influenced CH_4 emissions (Figure 4d,g). Plateauing trends were still observed with higher values of RAP, RLT, MMR and RMMC, even though these parameters had significant effects on emissions (Figures 1 and 4d). OAW was a highly influential parameter for CH_4 emissions with SFI > 0.3 (Figure 4e), while WCI and HDC were also highly influential with SFI > 0.1 (Figure 4e).

3.2.3. Water Cycling

Both N_2O and CH_4 emissions are significantly influenced by parameters related to the drainage system (Figure 5). Higher values of each of the following parameters: minimum roughness length (MRL), runoff first order rate coefficient (RFO), correspond amount cover surface (CAC), maximum surface storage without causing runoff (MSS), and empirical scale in pore shape (ESP) had a clear influence on reducing in N_2O emissions (Figure 5a,e). MRL was the most influential parameter for emissions as SFI > 0.8, while the SFI values for MSS and ESP, which influenced emissions, were both greater than 0.4. However, interception storage capacity per LAI (ISC-LAI), precipitation N concentration (PRN), coefficient in water function (CWF) and drain pipe level (DPL) were found to be relatively sensitive to emissions, with SFI values ranging between 0.1 and 0.2. Simulated N_2O increased slightly across the full range of those values specified (Figure 5a–c).

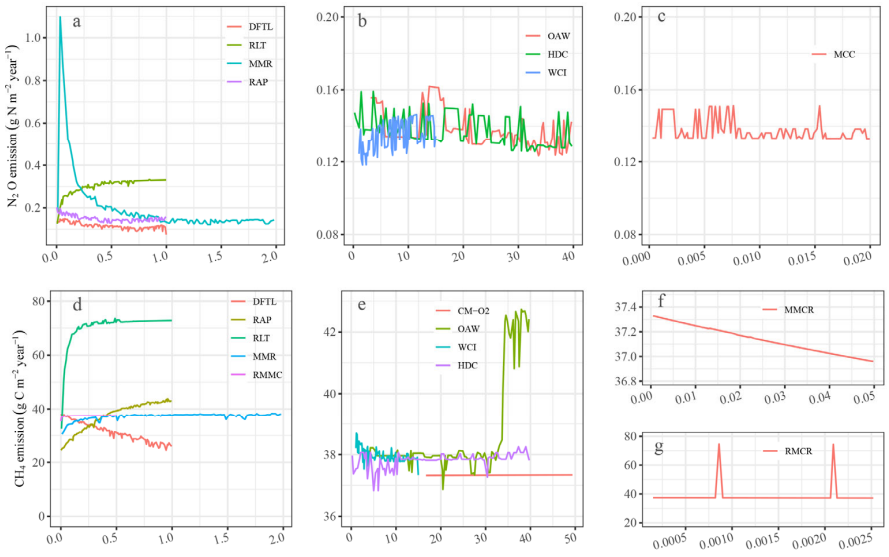

Figure 4. Relationship between N_2O and CH_4 emissions and various parameters: (**a**–**c**) carbon turnover and microbial respiration parameters, dissolved fraction in transferred litter (DFTL), residue to litter transfer rate (RLT), microbial maintenance respiration rate (MMR), relative activity at porosity (RAP); optimal available water content (OAW), half DOC concentration (HDC), water content interval to unity (WCI); maintenance coefficient on carbon (MCC); (**d**–**g**) carbon decomposition, oxygen regulation, and methane consumption parameters: DFTL, RAP, MMR, RLT, and rhizospheric Michaelis constant (RMMC); OAW, WCI, oxygen Michaelis constant (CM-O_2), HDC, maximum methane consumption rate (MMCR) and rhizospheric maximal methane consumption rate (RMCR).

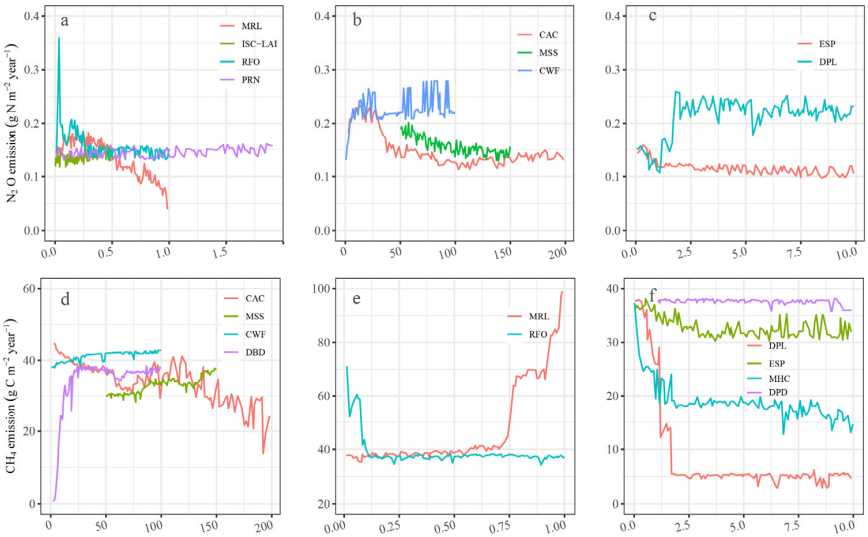

Figure 5. Changes in annual N_2O and CH_4 emissions in response to water cycling parameters: (**a**–**c**) showed that surface roughness, precipitation, and soil water regulation affected N_2O emissions, minimum roughness length (MRL), runoff first-order rate coefficient (RFO), interception storage capacity per leaf area index (ISC-LAI), and nitrogen concentration in precipitation (PRN); maximum surface storage without causing runoff (MSS), corresponding water amount to cover the surface (CAC), and coefficient in the water function (CWF); empirical scale in pore shape (ESP) and drain pipe level (DPL); (**d**–**f**) showed that surface storage, drainage, and hydraulic parameters affected CH_4 emissions, MSS, CWF, CAC, and distance between drainpipes (DBD); MRL and RFO; minimum hydraulic conductivity (MHC), DPL, ESP, and drain pipe diameter (DPD).

The simulation of annual CH_4 emissions was particularly sensitive to parameters CAC, MSS, CWF, distance between drainpipes (DBD), MRL, RFO, DPL, ESP, minimum hydraulic conductivity (MHC), and drain pipe diameter (DPD), with SFI values greater

than 0.1 (Figures 1 and 5d–f). MSS and CWF were the most sensitive parameters (SFI > 0.6) for emissions, with increases in CH_4 emissions observed when MSS and CWF less than 150 mm and 100 mm, respectively (Figure 5d). Substantial reductions in emissions were found for CAC (<200), MHC (<2), DPL (<2), ESP (<3) and RFO (<0.2), while MRL (>0.75) and DBD (<25 m) resulted in significant increases in emissions. Additionally, a stepped but small decline in CH_4 emissions was observed for DPD across its minimum to maximum specified values.

3.3. Soil Properties

To examine the contribution of soil properties to N_2O and CH_4 emissions, we present detailed results of eleven parameters related to soil physical-chemical characteristics at depths of 0–10 cm and 10–20 cm (Table 2). The changes in N_2O and CH_4 emissions corresponding to parameters with SFI > 0.1 are shown in Figure 6. Soil saturated water content had the greatest influence on the simulations for N_2O and CH_4 emissions (Figure 6a,d) with SFI values > 0.8 (Figure 1). For the simulated N_2O emissions, higher values of air entry pressure (AEPL1 and AEPL2), saturated matrix conductivity (SMCL1), and water content at the wilting point (WPL1) (Figure 6a), bulk density (DSBDL1, Figure 6b) and residual water content (RSWCL1, Figure 6c) resulted in reductions in emissions (Figure 6a). In contrary, emissions increased with higher values of soil saturated water content in the subsoil (SSCL2, Figure 6a), pores size distribution index (PSDIL1, Figure 6b), soil pH (PHL1, Figure 6c), which are related to the diffusion rate of N_2O, substrate availability and vertical water exchange in the soil profile. Similarly, four parameters related to soil properties, SSC (SSCL1 and SSCL2), air entry pressure (AEPL1 and AEPL2), SMCL1 and PHL1, were also influential (Figure 6d,f), with SFI values > 0.2. For RSWCL1 values between ca. 6 and 10 vol%, a stepped but modest increase in emissions was observed (Figure 6e).

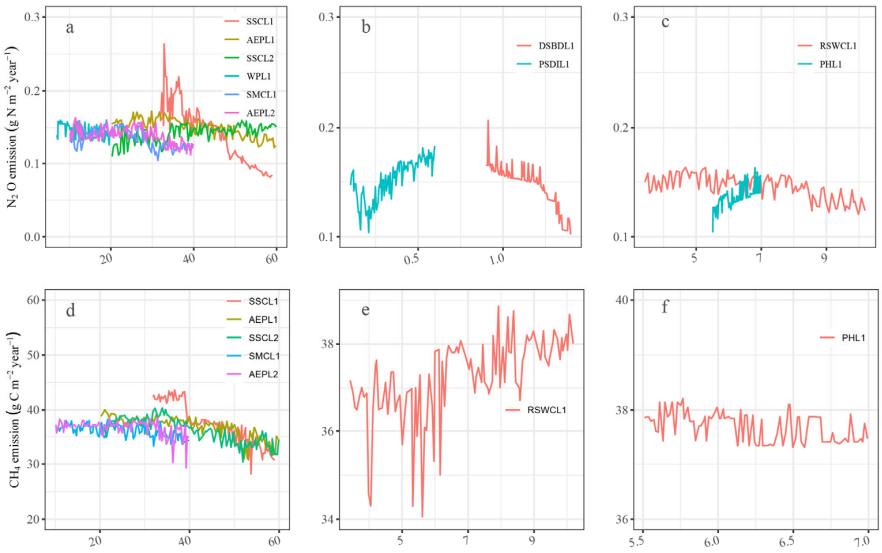

Figure 6. Changes in annual N_2O and CH_4 emissions with parameters related to soil properties. (**a**–**c**) Sensitivity responses of N_2O emissions to soil hydraulic and physicochemical properties: soil saturated water content at 0–10 cm (SWCL1), soil saturated water content at 10–20 cm (SWCL2), air entry pressure at 0–10 cm (AEPL1), air entry pressure at 10–20 cm (AEPL2), saturated matrix conductivity at 0–10 cm (SMCL1), and water content at the wilting point at 0–10 cm (WPL1); bulk density at 0–10 cm (DSBDL1) and pore size distribution index at 0–10 cm (PSDIL1);soil residue water content at 0–10 cm (RSWCL1) and soil pH at 0–10 cm (PHL1). (**d**–**f**) Sensitivity responses of CH_4 emissions to soil hydraulic and chemical properties: SWCL1, SWCL2, SMCL1, AEPL1, and AEPL2; RSWCL1; PHL1.

4. Discussion

4.1. Comparison with the Previous Study

This study builds upon the previous SA by Shan et al. [28], which focused on a single wheat season. However, our analysis focuses on conditions within a winter wheat–rice double cropping system, characterized by alternating wet and dry cycles, to highlight the impact of SWC and microbial activities on GHG emissions. This transition shifts N_2O responses to weather and fertilization during the upland wheat season, while amplifying CH_4 sensitivity during the flooded rice season. In addition, we assess the sensitivity of N_2O and CH_4 emissions to soil properties, weather conditions and fertiliser applications management. Importantly, the method adopted by this study differs from that used in the previous study.

The SFI is particularly effective for SA because it directly quantifies the contribution of each input variable/parameter to the overall variance in the model output, providing a clear understanding of the main effects of individual factors. Unlike simpler methods such as the Morris method or OAT analysis [36,37], which primarily focus on screening factors or provide only qualitative insights, the SFI offers a quantitative measure that captures both linear and non-linear effects of each input variable/parameter independently [25]. This capability is crucial for simulating complex processes in an agroecosystem, where interactions among variables can significantly impact the outputs. Moreover, the SFI excels at decomposing variance and providing detailed information about individual factors [35]. This precision and efficiency make the SFI particularly well-suited for large-scale models, where computational resources may be limited but a detailed understanding of each factor's influence is required.

4.2. Effects of Fertilisation, Weather, Soil and Model Process Parameters on N_2O and CH_4 Emissions

The type and timing of fertiliser application can significantly affect N_2O and CH_4 emissions. Chemical fertilisers increase soil mineral N availability, which can enhance nitrification and denitrification processes, leading to elevated N_2O emissions, especially under wet or anaerobic conditions [6,29]. Changes in N_2O emissions were markedly higher when more fertiliser was applied as topdressing (Figure 2a). This is consistent with the understanding that N-rich fertilisers enhance N_2O emissions by simulating these processes [38,39]

N_2O emissions are influenced by multiple factors, including N availability, dissolved organic carbon content, SWC and microorganisms, all of which vary both temporally and spatially [40–43]. Among the sixty-five parameters, HPD, ASF, MDG-NO_2, BTD, BTN, MRL, O_2IH, MDG-N_2O, MSS, RLT and DFTL are the most sensitive parameters for emissions (Figure 1). HPD, RLT and DFTL are related to the C substrate supplied by the decomposition of humus and litter. ASF represents the conversion efficiency of decomposed OM into microbial C, while BTN and BTD are related to the acceleration of nitrification and denitrification as soil temperature increases, leading to enhanced microbial activities. Their significant influence on N_2O emissions is in agreement with the previous findings that ASF, HPD, BTD and BTN are critical parameters for N_2O emission rates through microbial processes [28]. MDG-NO_2 and MDG-N_2O play a critical role in N_2O emissions by facilitating the conversion of nitrite intermediates and the reduction of N_2O by denitrifying bacteria, which is different from the previous study by Shan et al. [28]. MRL and MSS are key parameters for controlling water evaporation rates and waterlogging levels in a field, respectively. They influence the frequency of the dry-wet cycle, which in turn affects N_2O emissions through microbial pathways. The O_2IH parameter controls soil oxygen levels that significantly affect N_2O production, especially under low oxygen

concentrations when sufficient substrate is available [44]. However, lower SFI values (<0.1) for microbial parameters that control nitrification and denitrification processes, such as MNG, MGY-NO, PPF-N_2O, MAN, PPF-NO and MDG-NO, suggested a less significant impact on N_2O emissions (Figure 1). This may be attributed to the dynamic and complex interactions among SWC, microbial community composition, and weather conditions within the agroecosystem [45–47].

Our analysis indicated that simulated CH_4 emissions were most sensitive to changes in HPD, RMCR, MMCR, CM-O_2, O_2IH, BTM, DFTL, RAP and FLP with SFI values > 0.8 (Figure 1). The parameters HPD, FLP and DFTL had significant impacts on processes in soil C cycling, influencing the decomposition of OM transferred to the dissolved C pool, which subsequently affects emissions. RMCR, MMCR, CM-O_2 and O_2IH are key control factors for CH_4 consumption by both rhizospheric and soil methanotrophs. Reduced soil oxygen and a lower emission consumption rate favour methane-producing microbes while inhibiting aerobic respiration, ultimately resulting in increased CH_4 emissions [32]. Higher RAP values indicated more favourable conditions for methanogenic bacteria, leading to increased CH_4 production by enhancing substrate availability and regulating oxygen exchange through the control of soil pore structure [48]. Rising temperatures have been reported to contribute to increased CH_4 emissions [49,50]. However, our simulation results showed elevated air temperatures led to only a slight increase in CH_4 emissions (Figure 2c). This may be associated with the slow increase in soil temperature due to higher surface water evaporation rates during the rice growing period, which inhibits the rapid decomposition of organic matter.

4.3. Implications and Limitation

The identified sensitive parameters translate into clear management opportunities. Enhancing N management, particularly optimizing the basal/topdressing split, can mitigate N_2O surges during the aerobic wheat season. For the anaerobic rice phase, improved drainage scheduling can suppress CH_4 production linked to methanogenesis-sensitive parameters. Additionally, the strong temperature dependence of both gases suggests that practices influencing soil thermal regimes (e.g., residue management, controlled irrigation) may offer further emission reductions. Our findings reveal that parameters linked to microbial activities and weather conditions significantly affect N_2O and CH_4 emissions (Figure 1). This contrasts with earlier findings where soil conditions and management were considered more sensitive than weather conditions [28]. The alternation between growing dryland wheat and paddy rice alters microbial accessibility [51] and affects microbial structure and function due to the dry-wet cycles, likely favouring microbial taxa adapted to these dynamic conditions [52]. Sensitivity analysis using the same model across different cropping systems demonstrated variations in the controlling processes and conditions for N_2O and CH_4 emissions.

Although our findings on parameter sensitivity may have global applicability, several limitations warrant consideration. The sample size, consistent with the previous study [28], involved sampling each variable or parameter 100 times. To evaluate whether this density was sufficient, we conducted convergence tests by increasing the sample size to 200 and 500. The sensitivity rankings stabilized after approximately 100–150 samples, suggesting that the adopted sample size provides reliable estimates while balancing computational feasibility. Nonetheless, we acknowledge that larger sample sizes could further reduce uncertainty and may be considered in future studies. Additionally, the intricate interplay of multiple factors, such as SWC, temperature, and fertilization practices, adds complexity and often results in nonlinear interactions that vary depending on environmental contexts. While our analysis focused on temperature and rainfall as the primary climatic drivers for

this system, existing models may inadequately capture such complexities, particularly in regions with diverse climates or cropping systems [53,54]. Moreover, model uncertainty partly arises from the limited availability of empirical measurements for several highly sensitive parameters operating across both the wheat (aerobic) and rice (anaerobic) phases. Reducing this uncertainty will require prioritizing field measurements of parameters that strongly influence nitrification, denitrification, methanogenesis, and CH_4 oxidation, thereby improving model robustness in double-cropping systems.

5. Conclusions

Sobol's first-order method was used to quantitatively assess the effects of weather variations, soil properties, and fertilization on N_2O and CH_4 emissions, with a focus on identifying sensitive parameters in the process-based SPACSYS model for a winter wheat–rice double cropping system. Our results showed that the Sobol method effectively pinpointed key sensitive parameters, particularly those influencing gas emissions, such as SSCL, O_2IH, and those related to microbial processes. Both N_2O and CH_4 emissions were sensitive to parameters including HPD, O_2IH, and DFTL. Specifically, for N_2O emissions, additional influential factors included ASF, MDG-NO_2, BTD, BTN, MRL, MDG-N_2O, MSS, and RLT, all of which are associated with microbial processes and SWC. In contrast, CH_4 emissions were more sensitive to parameters related to CH_4 consumption, oxygen levels, and C substrates, including RMCR, MMCR, CM-O_2, BTM, RAP, and LFLP. Furthermore, fertilization, rainfall and temperature were found to be highly influential for N_2O emissions, while temperature was identified as the primary sensitive factor for CH_4 emissions. These findings highlight the critical role of environmental and management interactions in regulating GHG fluxes. They also suggest that future improvements should focus on integrating microbial community composition and functionality into parameterization strategies, as well as examining the interactive effects of weather, soil properties, and agricultural practices to enhance the robustness of sensitivity analyses and model calibration.

Supplementary Materials: The following supporting information can be downloaded at: https://www.mdpi.com/article/10.3390/agriculture16010011/s1. Table S1: Parameters on water, C and N processes for the sensitivity analysis, together with their default values.

Author Contributions: Conceptualization, C.L., Y.S. and L.W.; methodology, C.L., J.W. and L.W.; software, C.L. and L.W.; validation, C.L., Y.L. and L.W.; formal analysis, investigation and data curation, J.W., Z.S. and Y.S.; writing—original draft preparation, C.L., J.W., Y.S. and L.W.; writing—review and editing, C.L., Y.S., Y.L. and L.W.; visualization, J.W., Z.S. and C.L.; supervision, C.L., Y.S., Y.L. and L.W.; project administration and funding acquisition, C.L. and L.W. All authors have read and agreed to the published version of the manuscript.

Funding: This research was funded by the National Natural Science Foundation (Young Scientists Fund, 32201409), Ministry of Science and Technology of China (National High-end Foreign Expert Project, G2022019020L), Anhui Academy of Agricultural Sciences (Youg Backbone Talents Project, QNYC-202210) and China Scholarship Council (China–UK Joint Research and Innovation Partnership Fund PhD Placement Programme, 201802527008).

Data Availability Statement: Data related to the research are reported in the manuscript. Any additional data may be acquired from the corresponding author upon request.

Conflicts of Interest: The authors declare no conflicts of interest. The funders had no role in the design of the study; in the collection, analyses, or interpretation of data; in the writing of the manuscript; or in the decision to publish the results.

References

1. Zhang, G.; Ma, J.; Yang, Y.; Yu, H.; Song, K.; Dong, Y.; Lv, S.; Xu, H. Achieving low methane and nitrous oxide emissions with high economic incomes in a rice-based cropping system. *Agric. For. Meteorol.* **2018**, *259*, 95–106. [CrossRef]
2. Filonchyk, M.; Peterson, M.P.; Zhang, L.; Hurynovich, V.; He, Y. Greenhouse gases emissions and global climate change: Examining the influence of CO_2, CH_4, and N_2O. *Sci. Total Environ.* **2024**, *935*, 173359. [CrossRef] [PubMed]
3. Waha, K.; Dietrich, J.P.; Portmann, F.T.; Siebert, S.; Thornton, P.K.; Bondeau, A.; Herrero, M. Multiple cropping systems of the world and the potential for increasing cropping intensity. *Glob. Environ. Change* **2020**, *64*, 102131. [CrossRef] [PubMed]
4. Zhang, L.; Zhang, F.; Zhang, K.; Liao, P.; Xu, Q. Effect of agricultural management practices on rice yield and greenhouse gas emissions in the rice–wheat rotation system in China. *Sci. Total Environ.* **2024**, *916*, 170307. [CrossRef]
5. Zhang, Y.; Sheng, J.; Wang, Z.; Chen, L.; Zheng, J. Nitrous oxide and methane emissions from a Chinese wheat–rice cropping system under different tillage practices during the wheat-growing season. *Soil Tillage Res.* **2015**, *146*, 261–269. [CrossRef]
6. Liu, D.; Ma, C.; Liu, Y.; Mo, Q.; Lin, W.; Li, W.; Li, H.; Yang, B.; Ding, R.; Shayakhmetoya, A.; et al. Driving soil N_2O emissions under nitrogen application by soil environmental factor changes in garlic-maize rotation systems. *Eur. J. Agron.* **2024**, *156*, 127167. [CrossRef]
7. Smith, K.; Thomson, P.; Clayton, H.; Mctaggart, I.; Conen, F. Effects of temperature, water content and nitrogen fertilisation on emissions of nitrous oxide by soils. *Atmos. Environ.* **1998**, *32*, 3301–3309. [CrossRef]
8. Weitz, A.; Linder, E.; Frolking, S.; Crill, P.; Keller, M. N_2O emissions from humid tropical agricultural soils: Effects of soil moisture, texture and nitrogen availability. *Soil Biol. Biochem.* **2001**, *33*, 1077–1093. [CrossRef]
9. Qiu, Q.; Wu, L.; Ouyang, Z.; Li, B.; Xu, Y.; Wu, S.; Gregorich, E. Effects of plant-derived dissolved organic matter (DOM) on soil CO_2 and N_2O emissions and soil carbon and nitrogen sequestrations. *Appl. Soil Ecol.* **2015**, *96*, 122–130. [CrossRef]
10. Deng, X.; Xu, T.; Xue, L.; Hou, P.; Xue, L.; Yang, L. Effects of warming and fertilization on paddy N_2O emissions and ammonia volatilization. *Agric. Ecosyst. Environ.* **2023**, *347*, 108361. [CrossRef]
11. Danilova, O.V.; Suzina, N.E.; Van De Kamp, J.; Svenning, M.M.; Bodrossy, L.; Dedysh, S.N. A new cell morphotype among methane oxidizers: A spiral-shaped obligately microaerophilic methanotroph from northern low-oxygen environments. *ISME J.* **2016**, *10*, 2734–2743. [CrossRef]
12. Nwokolo, N.L.; Enebe, M.C. Methane production and oxidation—A review on the pmoA and mcrA genes abundance for understanding the functional potentials of the agricultural soil. *Pedosphere* **2025**, *35*, 161–181. [CrossRef]
13. Larios, A.D.; Brar, S.K.; Ramírez, A.A.; Godbout, S.; Sandoval-Salas, F.; Palacios, J.H. Challenges in the measurement of emissions of nitrous oxide and methane from livestock sector. *Rev. Environ. Sci. Biotechnol.* **2016**, *15*, 285–297. [CrossRef]
14. Merino, A.; Pérez-Batallón, P.; Macías, F. Responses of soil organic matter and greenhouse gas fluxes to soil management and land use changes in a humid temperate region of southern Europe. *Soil Biol. Biochem.* **2004**, *36*, 917–925. [CrossRef]
15. Butterbach-Bahl, K.; Papen, H.; Rennenberg, H. Impact of gas transport through rice cultivars on methane emission from rice paddy fields. *Plant Cell Environ.* **1997**, *20*, 1175–1183. [CrossRef]
16. Roth, F.; Sun, X.; Geibel, M.C.; Prytherch, J.; Brüchert, V.; Bonaglia, S.; Broman, E.; Nascimento, F.; Norkko, A.; Humborg, C. High spatiotemporal variability of methane concentrations challenges estimates of emissions across vegetated coastal ecosystems. *Glob. Change Biol.* **2022**, *28*, 4308–4322. [CrossRef]
17. Muller, B.; Martre, P. Plant and crop simulation models: Powerful tools to link physiology, genetics, and phenomics. *J. Exp. Bot.* **2019**, *70*, 2339–2344. [CrossRef]
18. Wu, L. *SPACSYS (v6.00)—Installation and Operation Manual*; Rothamsted Research: North Wyke, UK, 2019; Available online: http://www.rothamsted.ac.uk (accessed on 15 April 2025).
19. Wu, L.; Wu, L.; Bingham, I.J.; Misselbrook, T.H. Projected climate effects on soil workability and trafficability determine the feasibility of converting permanent grassland to arable land. *Agric. Syst.* **2022**, *203*, 103500. [CrossRef]
20. Bingham, I.J.; Wu, L. Simulation of wheat growth using the 3D root architecture model SPACSYS: Validation and sensitivity analysis. *Eur. J. Agron.* **2011**, *34*, 181–189. [CrossRef]
21. Zhang, X.; Xu, M.; Liu, J.; Sun, N.; Wang, B.; Wu, L. Greenhouse gas emissions and stocks of soil carbon and nitrogen from a 20-year fertilised wheat-maize intercropping system: A model approach. *J. Environ. Manag.* **2016**, *167*, 105–114. [CrossRef]
22. Liu, C.; Wang, L.; Le Cocq, K.; Chang, C.; Li, Z.; Chen, F.; Liu, Y.; Wu, L. Climate change and environmental impacts on and adaptation strategies for production in wheat-rice rotations in southern China. *Agric. For. Meteorol.* **2020**, 292–293, 108136. [CrossRef]
23. DeJonge, K.C.; Ascough, J.C.; Ahmadi, M.; Andales, A.A.; Arabi, M. Global sensitivity and uncertainty analysis of a dynamic agroecosystem model under different irrigation treatments. *Ecol. Model.* **2012**, *231*, 113–125. [CrossRef]
24. Ma, H.; Wang, J.; Liu, T.; Guo, Y.; Zhou, Y.; Yang, T.; Zhang, W.; Sun, C. Time series global sensitivity analysis of genetic parameters of CERES-maize model under water stresses at different growth stages. *Agric. Water Manag.* **2023**, *275*, 108027. [CrossRef]
25. Pianosi, F.; Beven, K.; Freer, J.; Hall, J.W.; Rougier, J.; Stephenson, D.B.; Wagener, T. Sensitivity analysis of environmental models: A systematic review with practical workflow. *Environ. Model. Softw.* **2016**, *79*, 214–232. [CrossRef]

26. Saltelli, A.; Ratto, M.; Andres, T.; Campolongo, F.; Cariboni, J.; Gatelli, D.; Saisana, M.; Tarantola, S. *Introduction to Sensitivity Analysis, Global Sensitivity Analysis. The Primer*; John Wiley & Sons, Ltd.: Chichester, UK, 2007; pp. 1–51. [CrossRef]
27. Vanuytrecht, E.; Raes, D.; Willems, P. Global sensitivity analysis of yield output from the water productivity model. *Environ. Model. Softw.* **2014**, *51*, 323–332. [CrossRef]
28. Shan, Y.; Huang, M.; Harris, P.; Wu, L. A Sensitivity Analysis of the SPACSYS Model. *Agriculture* **2021**, *11*, 624. [CrossRef]
29. Liu, C.; Sun, Z.; Wang, X.; Wu, G.; Yuan, M.; Wang, J.; Sun, Y.; Liu, Y.; Wu, L. Optimizing fertilization strategies for a climate-resilient rice–wheat double cropping system. *Nutr. Cycl. Agroecosyst.* **2024**, *129*, 21–35. [CrossRef]
30. WRB IUSS Working Group. *World Reference Base for Soil Resources 2014, Update 2015 International Soil Classification System for Naming Soils and Creating Legends for Soil Maps*; World Soil Resources Reports 2015, No. 106; FAO: Rome, Italy, 2015.
31. Wu, L.; McGechan, M.; McRoberts, N.; Baddeley, J.; Watson, C. SPACSYS: Integration of a 3D root architecture component to carbon, nitrogen and water cycling—Model description. *Ecol. Model.* **2007**, *200*, 343–359. [CrossRef]
32. Sabrekov, A.F.; Glagolev, M.V.; Alekseychik, P.K.; Smolentsev, B.A.; Terentieva, I.E.; Krivenok, L.A.; Maksyutov, S.S. A process-based model of methane consumption by upland soils. *Environ. Res. Lett.* **2016**, *11*, 075001. [CrossRef]
33. Raivonen, M.; Smolander, S.; Backman, L.; Susiluoto, J.; Aalto, T.; Markkanen, T.; Mäkelä, J.; Rinne, J.; Peltola, O.; Aurela, M.; et al. HIMMELI v1.0: HelsinkI Model of MEthane buiLd-up and emIssion for peatlands. *Geosci. Model Dev.* **2017**, *10*, 4665–4691. [CrossRef]
34. Susiluoto, J.; Raivonen, M.; Backman, L.; Laine, M.; Makela, J.; Peltola, O.; Vesala, T.; Aalto, T. Calibrating the sqHIMMELI v1.0 wetland methane emission model with hierarchical modeling and adaptive MCMC. *Geosci. Model Dev.* **2018**, *11*, 1199–1228. [CrossRef]
35. Sobol, I.M. Global sensitivity indices for nonlinear mathematical models and their Monte Carlo estimates. *Math. Comput. Simul.* **2001**, *55*, 271–280. [CrossRef]
36. Morris, M.D. Factorial Sampling Plans for Preliminary Computational Experiments. *Technometrics* **1991**, *33*, 161–174. [CrossRef]
37. van Griensven, A.; Meixner, T.; Grunwald, S.; Bishop, T.; Diluzio, M.; Srinivasan, R. A global sensitivity analysis tool for the parameters of multi-variable catchment models. *J. Hydrol.* **2006**, *324*, 10–23. [CrossRef]
38. Lourenço, K.S.; Cantarella, H.; Soares, J.R.; Gonzaga, L.C.; Menegale, P.L.d.C. DMPP mitigates N_2O emissions from nitrogen fertilizer applied with concentrated and standard vinasse. *Geoderma* **2021**, *404*, 115258. [CrossRef]
39. Pan, S.-Y.; He, K.-H.; Lin, K.-T.; Fan, C.; Chang, C.-T. Addressing nitrogenous gases from croplands toward low-emission agriculture. *npj Clim. Atmospheric Sci.* **2022**, *5*, 43. [CrossRef]
40. Hénault, C.; Grossel, A.; Mary, B.; Roussel, M.; Léonard, J. Nitrous Oxide Emission by Agricultural Soils: A Review of Spatial and Temporal Variability for Mitigation. *Pedosphere* **2012**, *22*, 426–433. [CrossRef]
41. Basche, A.D.; Miguez, F.E.; Kaspar, T.C.; Castellano, M.J. Do cover crops increase or decrease nitrous oxide emissions? A meta-analysis. *J. Soil Water Conserv.* **2014**, *69*, 471. [CrossRef]
42. Eash, L.; Ogle, S.; McClelland, S.C.; Fonte, S.J.; Schipanski, M.E. Climate mitigation potential of cover crops in the United States is regionally concentrated and lower than previous estimates. *Glob. Change Biol.* **2024**, *30*, e17372. [CrossRef]
43. Rautakoski, H.; Korkiakoski, M.; Mäkelä, J.; Koskinen, M.; Minkkinen, K.; Aurela, M.; Ojanen, P.; Lohila, A. Exploring temporal and spatial variation of nitrous oxide flux using several years of peatland forest automatic chamber data. *Biogeosciences* **2024**, *21*, 1867–1886. [CrossRef]
44. Wrage, N.; Velthof, G.L.; van Beusichem, M.L.; Oenema, O. Role of nitrifier denitrification in the production of nitrous oxide. *Soil Biol. Biochem.* **2001**, *33*, 1723–1732. [CrossRef]
45. Oorts, K.; Merckx, R.; Gréhan, E.; Labreuche, J.; Nicolardot, B. Determinants of annual fluxes of CO_2 and N_2O in long-term no-tillage and conventional tillage systems in northern France. *Soil Tillage Res.* **2007**, *95*, 133–148. [CrossRef]
46. Grados, D.; Kraus, D.; Haas, E.; Butterbach-Bahl, K.; Olesen, J.E.; Abalos, D. Common agronomic adaptation strategies to climate change may increase soil greenhouse gas emission in Northern Europe. *Agric. For. Meteorol.* **2024**, *349*, 109966. [CrossRef]
47. Heimsch, L.; Vira, J.; Fer, I.; Vekuri, H.; Tuovinen, J.-P.; Lohila, A.; Liski, J.; Kulmala, L. Impact of weather and management practices on greenhouse gas flux dynamics on an agricultural grassland in Southern Finland. *Agric. Ecosyst. Environ.* **2024**, *374*, 109179. [CrossRef]
48. Conrad, R. Microbial Ecology of Methanogens and Methanotrophs. *Adv. Agron.* **2007**, *96*, 1–63. [CrossRef]
49. Rowlings, D.W.; Grace, P.R.; Kiese, R.; Weier, K.L. Environmental factors controlling temporal and spatial variability in the soil-atmosphere exchange of CO_2, CH_4 and N_2O from an Australian subtropical rainforest. *Glob. Change Biol.* **2011**, *18*, 726–738. [CrossRef]
50. Cheng, C.-H.; Redfern, S.A.T. Impact of interannual and multidecadal trends on methane-climate feedbacks and sensitivity. *Nat. Commun.* **2022**, *13*, 3592. [CrossRef]
51. Luo, S.; Jia, Z.; Tian, L.; Wang, S.; Chang, C.; Ji, L.; Chang, J.; Zhang, J.; Tian, C. Potential functional differentiation from microbial perspective under dryland-paddy conversion in black soils. *Agric. Ecosyst. Environ.* **2023**, *353*, 108562. [CrossRef]

52. Gu, Y.; Zhang, X.; Tu, S.; Lindström, K. Soil microbial biomass, crop yields, and bacterial community structure as affected by long-term fertilizer treatments under wheat-rice cropping. *Eur. J. Soil Biol.* **2009**, *45*, 239–246. [CrossRef]
53. Daron, J.D.; Sutherland, K.; Jack, C.; Hewitson, B.C. The role of regional climate projections in managing complex socio-ecological systems. *Reg. Environ. Change* **2014**, *15*, 1–12. [CrossRef]
54. Gonçalves, B.; Morais, M.C.; Pereira, S.; Mosquera-Losada, M.R.; Santos, M. Tree–Crop Ecological and Physiological Interactions Within Climate Change Contexts: A Mini-Review. *Front. Ecol. Evol.* **2021**, *9*, 661978. [CrossRef]